Chlorophyll and pheophytin protonated and deprotonated ions: Observation and theory

M. Diop, M. El-Hayek, J. Attard, A. Muhieddine, V. Veremeienko, S. Soorkia, Philippe Carbonnière, Aurélien de la Lande, B. Soep, Niloufar Shafizadeh

Chlorophyll and Pheophytin Protonated and Deprotonated Ions: Observation and Theory

M. Diop[1], M. el-Hayek[2], J. Attard[2,3], A. Muhieddine[1], V. Veremeienko[4], S. Soorkia[1], Ph. Carbonnière[3], A. de la Lande[2], B. Soep[1], and N. Shafizadeh[1]

1-Institut des Sciences Moléculaires d'Orsay (ISMO), France
2- Université Paris Saclay, CNRS, Institut de Chimie Physique, UMR 8000, 91405, Orsay, France
3- Institut des sciences analytiques et de physico-chimie pour l'environnement et les materiaux (IPREM) Pau, France
4- Université Paris-Saclay, CEA, CNRS, Institute for Integrative Biology of the Cell (I2BC), 91198Gif-sur-Yvette, France

Corresponding author: niloufar.shafizadeh@universite-paris-saclay fr

Abstract

Pheophytin *a* and chlorophyll *a* have been investigated by electrospray mass spectrometry in the positive and negative modes, in view of the importance of the knowledge of their properties in photosynthesis. Pheophytin and chlorophyll are both observed intensely in the protonated mode and their main fragmentation route is the loss of their phytyl chain. Pheophytin is observed intact in the negative mode while under collisions it is primarily cleaved beyond the phytyl chain and loses the attaching propionate group. Chlorophyll is not detected in normal conditions in the negative mode but addition of methanol solvent molecule is detected. Fragmentation of this adduct forms primarily a product (-30 amu) that dissociates into dephytyllated deprotonated chlorophyll. Semi-empirical molecular dynamics calculations show that the phytyl chain is unfolded from the chlorin cycle in pheophytin *a* and folded in chlorophyll *a*. Density functional theory calculations have been conducted to locate the charges on protonated and deprotonated pheophytin *a* and chlorophyll *a* and have found the major location sites that are notably more stable in energy by more than 0.5 eV than the others. The deprotonation site is found identical for pheophytin *a* and the chlorophyll *a*-methanol adduct. This is in line with experiment and calculation locating the addition of methanol on a double bond of deprotonated chlorophyll *a*.

Introduction

Chlorophylls and pheophytins (Figure 1) are the actors of the charge separation in the Photosystem II reaction center driving photosynthesis. In view of describing precisely the physical-chemical properties of chlorophylls in the reaction center, the observation of isolated chlorophyll and pheophytin, which are at the heart of charge separation is an essential task. Therefore, mass spectrometric observations in the gas phase of chlorophyll ions have been achieved in their cationic forms,[1-7] using different ionization methods. In turn, negative ions have been observed less frequently by ionization with electrons from the fission of ^{252}Cf [8, 9] or by electrospray.[10] The spectroscopic properties of isolated chlorophylls in absence of a perturbing medium leads to a direct comparison of the properties with calculations and calculations at the Density Functional Theory (DFT) level have been conducted previously on protonated forms but have not been done to our knowledge on negative ions.

Positively charged chlorophylls are formed with addition of quaternary ammonium[1-6] or simply protonation.[7, 11] These charges induce a strong shift in the absorption/emission properties of gas phase chlorophylls although the global fluorescence emission structure remains intact and similar to that of solutions.[11] We have sought to observe and characterize charged chlorophylls, typically deprotonated negatively charged with distant charges, inducing minimum perturbations to the active chlorin ring. Indeed the Q bands of deprotonated pheophytin in basic solutions are quasi identical to that of neutral chlorophyll.[12] Therefore, we have investigated their negative ions where the charge is likely to be located away from the chlorin ring. Here we have investigated in an electrospray source deprotonated chlorophyll *a* and pheophytin *a*, their dissociation by collisions and the formation and dissociation of related negative ions. DFT calculations have allowed to assess the localization of positive and negative charges on these systems. One of the conclusions of this work is that the solvent methanol adds to chlorophyll in negative ions in a mechanism similar to that observed by other authors in the deprotonation of weakly acidic species.[13] More generally in negative ions electrospray addition reactions can proceed in the droplets to electron deficient regions of parent molecules.[14, 15] This methanol addition is found favorable on chlorophyll *a* by DFT calculations.

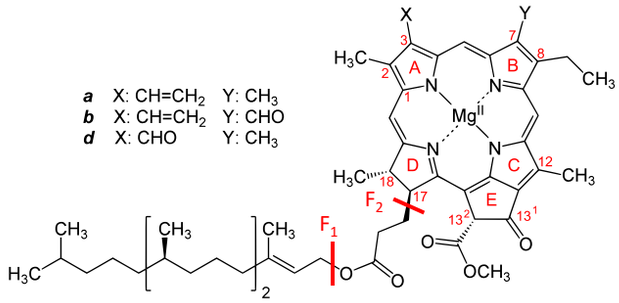

Figure 1 chlorophylls a, b, d and the two main cleavage locations F1 and F2. The corresponding pheophytin molecules have the central Mg atom replaced by two H atoms on opposite N(A) and N(C) atoms.

Experimental and computational methods

Electrospray from methanol solutions of chlorophyll *a* and pheophytin *a* have been conducted in the positive and negative modes forming protonated and deprotonated ions respectively. Solutions have been prepared at concentrations of 10^{-5} mol.L^{-1} from purified pigments by column chromatography with the addition of a drop of ammonia.

Purification of pheophytin a. The conversion of chlorophylls into pheophytin and subsequent purification was done using a variation of published protocols.[16, 17] Briefly, a mixture comprising 100 g of spinach leaves was combined with 200 mL of water and 100 mL of acetone (Sigma Aldrich, purity ≥99 %), and grounded for 2 minutes. This process was repeated three times. The resulting paste was filtered through a filter paper 313 (VWR European Cat. No. 516-0806, size: 125 mm). Acetone was removed from the acetone/water mixture using a rotavap apparatus at 40 °C to further extract the pigments by liquid-liquid separation using dichloromethane (Sigma Aldrich, purity ≥99,8%). The organic fraction was filtered using a 200 nm Millipore filter and dried using a rotavap apparatus at 40 °C. A 40 mL of acetone/water mixture (75/25, v/v) was added to the dried sample and the pH was adjusted to 3 using HCl to demetallate the Chlorophyll *a*. Acetone was removed using a rotavap apparatus at 40 °C, and pigments extracted using 50 mL of dichloromethane by liquid-liquid separation. Finally, a column chromatography was run using as a stationary phase silica gel (Kieselgel 60, 0,02-0,045 mm) and mobile phase n-hexane/acetone (90/10, v/v).

A LCQ DECA XP Plus ion trap mass spectrometer (Thermo/Finnigan) was used to produce the positive or negative ions of the title compounds and conduct energy-controlled dissociations of chlorophyll *a* either in the source or in the trap. In the source, collisions are performed by

changing the skimmer/capillary voltage difference, thus providing an electrostatic laboratory collision energy that is converted in the center of mass energy of the N_2-molecule pair. The electrostatic energy is provided by a standard procedure in the Thermo Finnigan package, while in the trap collisions only provide a relative energy. However, the latter collisions relate directly and specifically to mass selected ions. Mass calibrations were performed with the sodium salt of microperoxidase (MP-11) and its fragments, purchased from Sigma Aldrich.

We carried out quantum chemistry calculations at the DFT and the semi-empirical Parametric Method 6 (PM6-DH2) levels with corrections for dispersive and hydrogen bond interactions (the so-called DH2 correction scheme).[18,19,20] deMon2k was used for DFT calculations (version 6.2.2).[21] This program relies on variational density fitting to speed-up the calculation and reduce memory demand.[22] We chose to work with the PBE (Perdew, Burke, Ernzerhof)[23] or the B3LYP exchange correlation functionals.[24] The triple zeta TZVP basis set was used for all atoms with the exception of Mg for which a DZVP-GGA basis set was chosen.[25,26] The GEN-A2 basis set was chosen to expand the auxiliary electron density. Exchange-correlation contributions were obtained by numerical integration of the fitted electron density[27] over grids of very high accuracy (10^{-7} Ha in deMon2k's input standard notations).[28] Geometries were optimized with tight tolerance criteria of 5.10^{-5} Ha/bohr applied on energy gradients. The nature of the optimized structures was systematically verified by mean of analytical frequency calculations within the auxiliary density perturbation theory.[29] PM6-DH2 Born Oppenheimer Molecular Dynamics simulations (MD) have been carried out with Cuby4[30] interfaced with MOPAC2009[31].

Results and Discussion

Pheophytin *a*

Protonated ions of pheophytin *a* are detected intensely at m/z 871.6 for the most intense peak of the ^{12}C isotopologue and with loss of the phytyl chain at m/z 593.3. In turn, deprotonated pheophytin *a* is easily observed with the same solution at m/z 869.6 and an exact defect of 2 amu with respect to the protonated ions. This identifies unambiguously pheophytin *a* in the protonated and deprotonated forms, as shown in Figure 2.

Collisions in the trap are investigated to ensure the stability of the protonated and deprotonated molecules. While collisions cleave the $C_{20}H_{38}$ fragment (phytyl group –H) off protonated pheophytin *a* yielding m/z 593.3, in the deprotonated form they detach the entire chain including the propionate group to form m/z 519.3, see in Figure 1, i.e., cleavages F_1 and F_2. Note that protonated pheophytin *a* loses easily a neutral fragment of mass 278.3 amu, i.e., one H atom less than the phytyl chain of mass 279.3 amu, Figure 2a. This has been observed on chlorophyll *a* by Wei[32] and interpreted as an H-atom transfer from the phytyl to chlorophyllide to avoid the formation of unpaired electrons in both fragments. Also, in negative deprotonated pheophytin *a*, the loss of the complete chain observed in moderate source collisions conditions (Figure 2b) is accompanied by an H-transfer from it, cleaving off $C_{23}H_{43}O_2$–H of mass 350.3 amu. Breakdown curves of fragment formation is included in the supporting information (SI Figure 1). Investigating in the same conditions deprotonated pheophytin *b*, the same fragmentation pattern was observed with the abstraction of the whole chain (phytyl + propionate) and an H migration leading to the loss of a neutral fragment at mass 350.3 amu (see SI Figure 2).

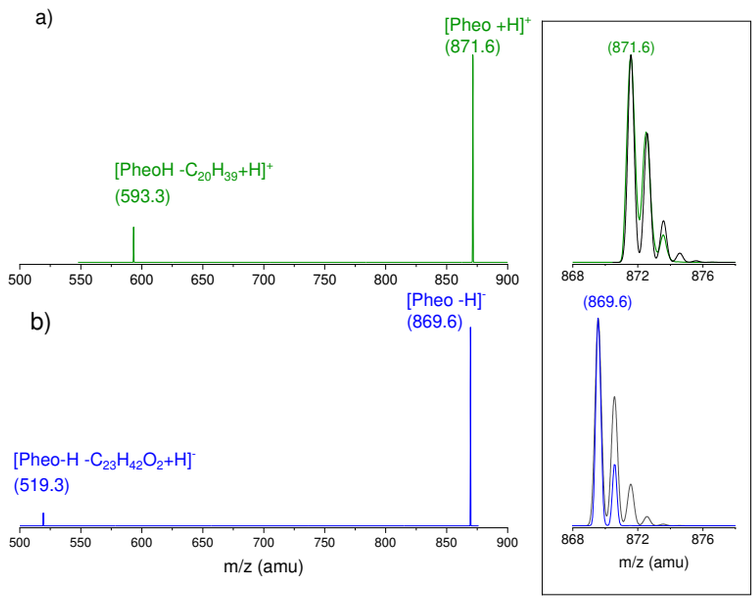

Figure 2 : mass spectra of protonated pheophytin a *(a) and deprotonated pheophytin* a*. On the right panel blowup views of the pheophytin mass domains displaying the isotopic distributions and their simulations (in gray color).*

Chlorophyll a

Protonated chlorophyll *a* is observed at m/z 893.6. It has been already characterized by Zvezdanovitch[7] and Wei,[32] who also studied its dissociation channels in details. Here, in-the-trap collisions also detach the phytyl chain of protonated chlorophyll *a* but leave a proton at the

end COO group, thus yielding m/z 615.4, as shows Figure 3a. This dephytilated fragment ion matches phytyl chain loss in pheophytin *a* with a (Mg-2H=22 amu) mass difference.

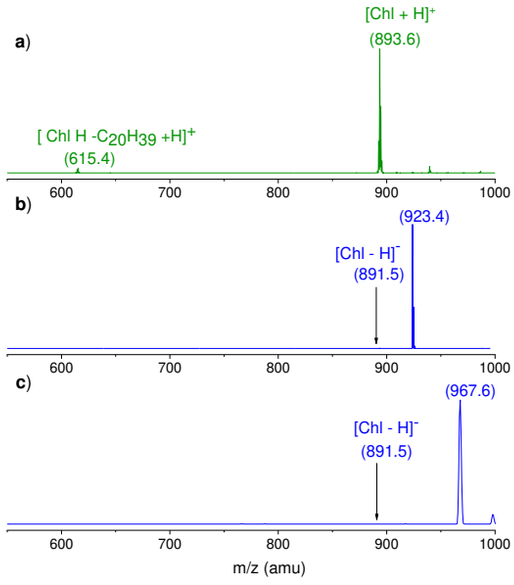

Figure 3 : Chlorophyll a: a) protonated species, b) negative species in methanol solvent c) negative species in a mixture of H_2O/propane-1,2-diol.

In difference with pheophytin *a*, deprotonated negative ions of chlorophyll *a* are generally not observed as shows Figure 3b and c. Instead, one monitors a new negative ion at m/z 923.4. This could match the addition of CH_3OH to deprotonated chlorophyll *a*. To test this hypothesis, we used a mixture of H_2O/propane1,2-diol (60/40) as a solvent in the electrospray. Then, the addition of $C_3H_8O_2H$ is also detected at m/z 967.6 amu as the dominant negative ion, confirming the previous hypothesis. Such alcohol molecule addition has already been observed in neutral solutions of chlorophyll *a* in methanol.[33]

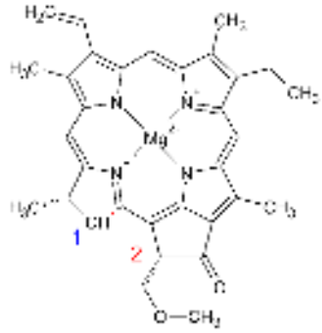

Figure 4: scheme of cleaved chlorophyll negative ion

When in trap collisions are applied to this selected methanol adduct, several products are observed. The first product to appear as a function of energy is m/z 893.3 amu differing by 30 amu from the parent at m/z 923.4, as can be seen in Figure 5a. It differs from deprotonated chlorophyll *a* by 2 mass units. This 'intermediate' can be prepared by in source collisions at 75 V and isolated in the trap as a monoisotopic species for resonant activation which yields the mass spectrum in Figure 5b. The main fragment is observed at m/z 613.9 amu that we assign to the loss of the phytyl chain producing deprotonated chlorophyllid *a* ($C_{35}H_{33}MgN_4O_5^-$, mass 613.23 amu). In this process we hypothesize that methanol was added on the chain (see the calculation section) on the phytyl double bond. The m/z 893.3 product loses CH_2O from the phytyl double bond, leaving it saturated. The dissociation of m/z 893.3 is deemed to form deprotonated chlorophyllid *a* with the loss of the chain but leaves an H atom at position 1 in Figure 4 on the propionic end. This avoids a radical fission as for protonated chlorophyll.[32]

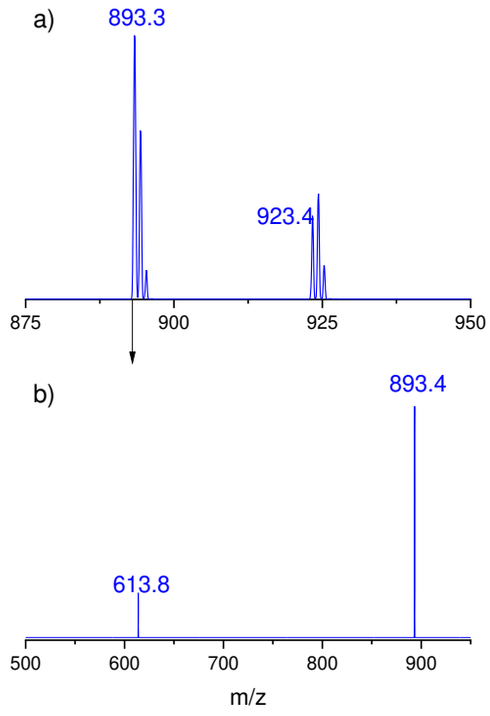

Figure 5: a) m/z 893.3 fragment of [Chl-H+32] was prepared by in-source collisions and it was isolated in a unit mass window separating the sole m/z 893.3 component. This m/z 893.3 mass component is then dissociated by resonant RF excitation with 20% reference energy to m/z 613.8. b) Plot of in trap dissociation of this adduct (m/z 893.3) monoisotopically selected with 1 amu width, in the 20-30% reference energy range.

In-trap dissociation has revealed that m/z 613.8 corresponds to dephytilated deprotonated chlorophyll *a*, equivalent to dephytilated protonated chlorophyll at m/z 615.4 (Figure 3a) with

two lesser H atoms. This is a strong indication that CH_3OH was added to the phytyl chain, since collisions have removed together with the phytyl chain, the two H atoms remnants on the 'intermediate' m/z 893.3 of the addition of methanol. However, these fragments although intense, are not the only ones. They serve here as markers of the structure of deprotonated chlorophyll *a*, as shows the computational study.

Computational Study

We have conducted theoretical calculations on chlorophyll *a* and pheophytin *a* to characterize the location of charges and the energetics of the charged isomers. We have considered two kinds of models, with or without the inclusion of the phytyl chain in the molecular system. To examine the protonation/deprotonation chemical sites, we considered a truncated model (i.e. without the phytyl chain), while for exploring the conformation of the phytyl chain with regard to the chlorophyll plane, we used a full system. In this scope, we explored the movements of the phytyl chain by molecular dynamics simulations to identify the shape of the potential energy surface. The simulations have highlighted the flexibility of the chain and the flatness of the potential energy surface and, as a consequence, the convergence of calculations becomes challenging. Furthermore, from experimental results the addition of methanol required to adopt the complete model to focus on the addition of methanol to the chain. We detail below the outcomes of our calculations.

Protonation/deprotonation sites on truncated models

DFT calculations have been carried out to locate charges on chlorophylls that are inaccessible to direct experiments. Essentially, the phytyl chain is replaced by a methyl group on the carboxyl functional group as (C=O)-O*CH₃* in Figure 6 at location 17,[4] to preserve the ester function of the full pigment. The relative DFT energies are reported in Figure 6 and Table 1. They include the zero-point-energy corrections.

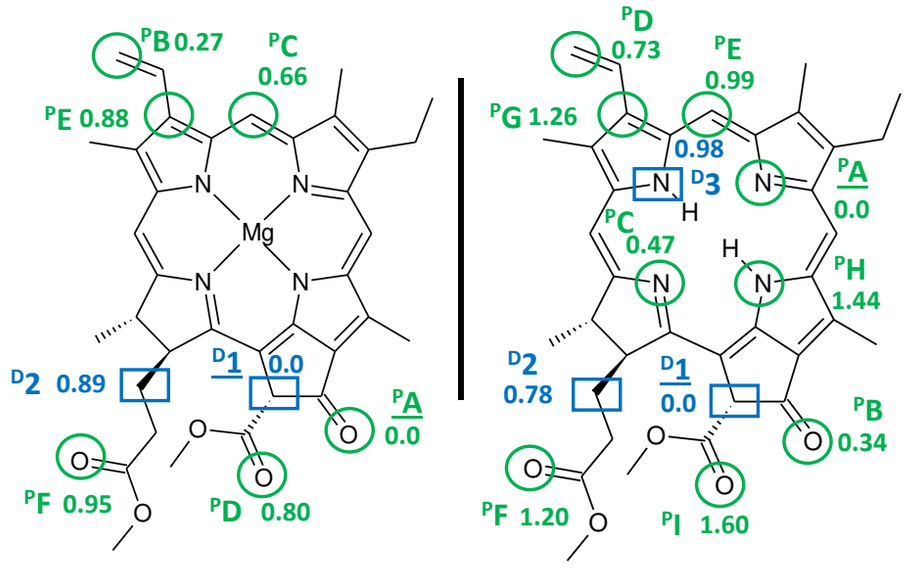

Figure 6 : truncated models of neutral chlorophyll a (left) and pheophytin a (right). The green circles indicate the protonation sites (^{P}X) with their relative stabilities with respect to conformer ^{P}A. The blue rectangles illustrate the tested deprotonation sites (^{D}Y), with their relative stabilities with respect to conformer ^{D}1. The relative energies are given in eV.

For chlorophyll *a*, we compared the relative stability of six protonation sites (^{P}A to ^{P}F, in green on the left-hand-side Figure 6, with labels P for protonation and D for deprotonation), taking structure ^{P}A as a reference. Protonation on the ketone function (site ^{P}A) is the most favorable protonation site (Figure 6). It is associated to a favorable protonation energy of -10.54 eV with respect to the energy of neutral chlorophyll *a*. Site ^{P}A is followed by site ^{P}B (vinyl function), 0.27 eV above in energy. Protonation on the carbonyl oxygen of the ester functions is much higher in energy than ^{P}A (0.80 and 0.95 eV for sites ^{P}D and ^{P}F respectively). Single point calculations with B3LYP on the PBE optimized structures gives the same stability ordering.

We have carried out a similar investigation for protonated pheophytin *a* and for sites ^{P}A-^{P}F, the ordering is the same, *but the lowest protonation site is located on a pyrrole nitrogen atom.* In addition to the six protonation sites discussed above, the replacement of the Mg^{2+} cation by two protons in pheophytin *a* leaves the possibility of three other protonation sites (^{P}A, ^{P}C and ^{P}H, Figure 6, right and Table 1). In fact, protonation of one pyrrole nitrogen atom (site ^{P}A) offers the most stable protonated species, before site ^{P}B. The protonation energy at site ^{P}A, including zero-point energy, is evaluated to -10.81 eV with the PBE functional.

Table 1 : Relative energies (in eV) of truncated chlorophyll a and pheophytin a ions (P for protonated, positive, D for deprotonated negative), obtained with the PBE functional. The numbers in brackets correspond to values obtained on the full model.

Sites	Chlorophyll *a*	Pheophytin *a*
^{P}A+	0.0	0.0
^{P}B	0.27	0.34
^{P}C	0.66	0.47
^{P}D	0.80	0.73
^{P}E	0.88	0.99
^{P}F	0.95	1.20
^{P}G	X	1.26
^{P}H	X	1.44
^{P}I	X	1.60
^{D}1-	0.0	0.0 (0.0)
^{D}2	0.89	0.78 (0.70)
^{D}3	X	0.98

Deprotonated species

In the deprotonation processes, we start with the truncated models showed in Figure 6. For chlorophyll, we have considered deprotonation on either one of the two alpha positions carbons of the ester (sites ^{D}1 and ^{D}2, blue rectangles) and found a clear preference of deprotonation for ^{D}1. This order is the same for pheophytin, except that a third deprotonation possibility is expected on the N-H functions (site ^{D}3). This however leads to a higher deprotonation energy, as shown in Figure 6 : truncated models of neutral chlorophyll a (left) and pheophytin a (right). The green circles indicate the protonation sites (^{PX}) with their relative stabilities with respect to conformer ^{PA}. The blue rectangles illustrate the tested deprotonation sites (^{DY}), with their relative stabilities with respect to conformer $^{D1.}$ The relative energies are given in eV.

Experimentally, a different direct deprotonation scheme is observed for chlorophyll leading to the facile formation of the adduct [Chla-MeO]$^{-}$, seemingly a lower energy route.

Conformational exploration of full molecular models

The addition of methanol on chlorophyll a is exothermic by a minimum of 0.5 eV on chlorophyll *a* (see below Table 3), in accordance with the observation of the methanol adduct. With the aim to investigate methanol addition, we have considered a larger, non-truncated, model for both chlorophyll *a* and pheophytin *a*, that explicitly includes the phytyl chain. The conformational space sampled by the chain has been explored by means of four 80 ps Born-Oppenheimer MD simulations carried out at the PM6-DH2 level of calculations (see Methods section) with random initial velocities and a temperature fixed at 300 K. We will refer to them as MD-X (X=1, 2, 3 or 4). The four starting structures were generated manually so as to vary the conformation of the chain. MD-1, 2 and 3 correspond to folded structures, while MD-4 correspond to a fully unfolded one, with the phytyl chain being completely elongated. We clustered the structures sampled by the simulations with the WMC physbio clustering tool [34] from VMD[35] based on the Root-Mean-Square-Deviation on the heavy atom positions. This tool gathers similar configurations into several cluster of configurations. Representative structures of each of the five most populated clusters have been extracted and re-optimized at the PM6-DH2 level[18,19,20] for each MD simulation. The cartesian coordinates of the most stable structures can be found in SI. The relative energies of the conformers generated by this procedure are collected in Table2 and labelled as clusters 1 to 5. The most stable folded and unfolded structures are represented in Figure 7.

For chlorophyll *a*, we find several folded conformers of similar energy within 0.1 eV. The unfolded ones lie 0.17 eV above the most stable one, which is the folded conformer. It is thus likely that some weak interactions between the phytyl groups and the magnesium cation could favour folded structures. More precisely, some interactions are expected between the Mg cation and the phytyl's double C=C bond in view of the short Mg-C distances of 2.66 and 2.88 Å seen in the most stable structure. The situation is reversed for pheophytin for which the fully elongated conformers are more stable by a fraction of an eV. To investigate solvent addition both on chlorophyll's C=C bonds, we have considered both folded and elongated form. It should be noted though that solvent addition removes the unsaturation, hence, the source of stability of the folded structures. Actually, after geometry optimization of the methanol adduct, we observe partial unfolding of the structure. To avoid unnecessary multiplications of tedious geometry optimizations, we focus in the following on addition of the fully unfolded structure.

Table 2 : Relative energies (in eV) of full chlorophyll a and pheophytin a models with their phytyl chain. MD-X corresponds to independent PM6-DH2 MD trajectories.

	Cluster of configurations				
Chlorophyll *a*	1	2	3	4	5
MD-1	0.07	0.36	0.28	0.45	0.40
MD-2	0.20	0.25	0.21	0.12	0.27
MD-3	0.06	0.09	0.11	**0.00**	0.16
MD-4	0.17	0.36	0.29	0.46	0.36
Pheophytin *a*					
MD-1	0.12	0.11	0.14	0.05	0.10
MD-2	0.12	0.10	0.11	0.18	0.14
MD-3	0.08	0.19	0.12	0.21	0.24
MD-4	**0.00**	0.06	0.03	0.01	0.07

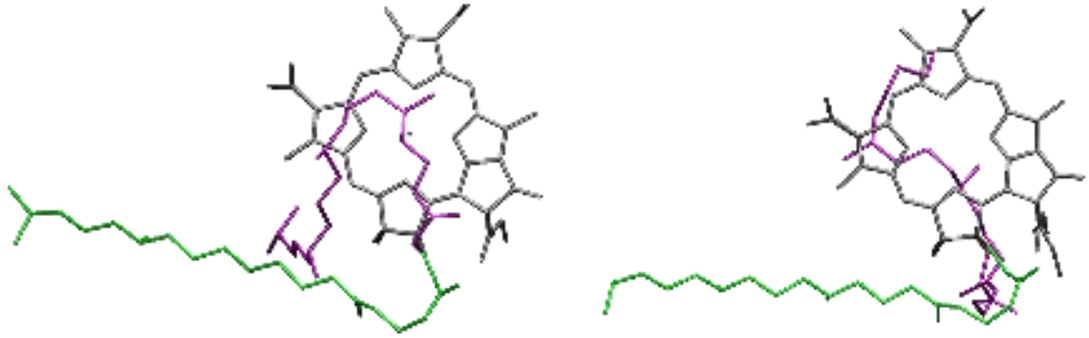

Figure 7 : Chlorophyll MD simulations The most stable structure, MD-1 (magenta) is folded, while MD-4 (green) is higher in energy .b) conformational sampling of the phytyl chain for pheophytin a. The most stable structure, MD-4 (green) is unfolded, and MD-1 (magenta) is higher in energy

In complement to these results, we have evaluated the relative energies of the deprotonated forms $^{D}1$ and $^{D}2$ (Table 1) for the large model pheophytin at the DFT level. The relative order is similar (separation 0.68 eV), and rather close to the energy found above with the truncated model (0.78 eV, see Table 1). This result validates *a posteriori* the truncated model used in the previous section to determine the most probable deprotonation sites. Also, this indicates that

the deprotonation sites are decoupled from the phytyl chain and can be considered independently.

Methanol addition

Based on experimental results, it seems there is an energy >1.6 eV for the formation of free deprotonated chlorophyll *a* from the its methoxy adduct, corresponding to a stable compound behind a possible barrier to methanol addition. There are several schemes that could explain the observation of this chlorophyll *a* adduct: either a methanolate anion (CH_3O^-) is added on neutral chlorophyll or a methanol molecule is added on already deprotonated chlorophyll *a*.

Relating to methanolate addition, it has been observed by Cole et al.[13, 36] that one route to the formation of anions in the absence of a 'strong' acidic site, is the addition of F^- or the acetate anion, wherefrom a deprotonated anion can be formed by in-source fragmentation of the $[M+A]^-$ adduct. Also, addition of CN^- on trinitrobenzene has been observed in the electrospray process[14]. The equivalent addition of methanolate anion is considered as unlikely due to its very low concentration in the methanol water solution in comparison with OH^-. Rather, one has to consider the addition of methanol on several double bonds of deprotonated chlorophyll *a*, on the lowest two deprotonated sites $^{D}1$ and $^{D}2$ represented in Figure 6. Their energies are listed in Table 3.

The addition of methanol on deprotonated $^{D}2$ and $^{D}1$ chlorophyll *a* has been calculated on double bonds ^{1}C-^{2}C and ^{3}C-^{4}C represented in orange in Figure 8. The site ^{1}C-^{2}C is found more favorable than ^{3}C-^{4}C for the addition, with $CH_3O^{\cdot}$ and $H^{\cdot}$ added preferably on ^{2}C and ^{1}C, respectively (see line line 4 in Table 3).

Furthermore, methanol addition on deprotonated chlorophyll *a* is more favorable on site $^{D}1$ than $^{D}2$ by 0.68 eV. On the other hand, in the case of $^{D}2$ deprotonation and ^{1}C addition (or $^{D}2$ - ^{2}C), one could consider a proton jump from the ^{1}C or ^{2}C atoms to the $^{D}2$ carbon atom, as illustrated in Figure 8 (inset, and entries $^{1}C + H^{+}$-^{2}D, $^{2}C + H^{+}$-^{2}D of Table 3). This proton transfer would stabilize the molecule, notably the $^{D}2$ - ^{1}C form, by 0.6 eV. The methanol added species in $^{D}2$

deprotonation are however higher in energy than the $^{D}1$ - ^{2}C form by 0.3eV, even after proton transfer, making the latter $^{D}1$ - ^{2}C combination, the most probable.

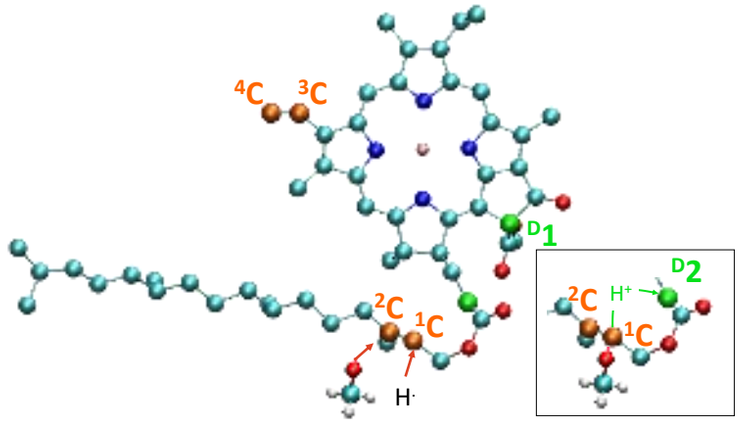

Figure 8 : Possible sites of methanol addition in orange, on a C=C double bond on the periphery of the chlorin ^{3}C-^{4}C or on the C=C the double bond of the phytyl chain ^{2}C-^{1}C. In the insert, $^{D}2$ deprotonation is followed by a proton transfer from ^{1}C localizing the negative charge on ^{1}C. The methanol addition in the combination $^{D}1$ - ^{2}C is shown below the chlorophyll molecule.

From experimental results, the addition of methanol likely occurs on the phytyl chain. There, the chain retains imprints of that addition with additional H atoms, which are suppressed when the phytyl is removed. Also, the collisions experiments indicate that the negative charge is not localized on the phytyl chain after dissociation.

*Table 3: Relative energies (in eV) of full chlorophyll and pheophytin a models including the phytyl chain and proton migration. * To compare energies of deprotonated and addition of methanol sites, we added the energy of optimized methanol to deprotonated sites energies as in line 1 and 2 of the table. ** Line (3) corresponds to the addition of $CH_3O^{\cdot}$ on ^{1}C and $H^{\cdot}$ on the contiguous ^{2}C and etc. *** The number in brackets correspond to the equivalent $^{D}1$ - ^{2}C adduct optimized for a folded structure.*

Sites of addition	Chlorophyll a (eV)	Pheophytin a (eV)
$^{D}1 + E_{MeOH}$	0.88*	0.94*
$^{D}2 + E_{MeOH}$	1.56*	1.64*
$^{D}1$ - ^{1}C	0.24	0.25
$^{D}1$ - ^{2}C	0 (0.28***)	0
$^{D}2$ - ^{1}C	0.91	1.09
$^{D}2$ - ^{2}C	0.80	0.96
$^{D}2$ - ^{3}C	1.01	1.21
$^{D}2$ - ^{4}C	1.08	1.26
$^{1}C + H^{+}$-^{2}D	0.30	0.34
$^{2}C + H^{+}$-^{2}D	0.65	0.72

Otherwise, fragmented chlorophyll would not be seen, in absence of charge relocation during the collision. In addition, $^{D}2$ adducts are all higher in energy than the corresponding $^{D}1$'s, making them unfavourable for methanol addition. As seen in Table 3, addition of methanol to ^{2}C forms the lowest energy deprotonated adduct with a stabilization energy of 0.88 eV with respect to free deprotonated $^{D}1$ chlorophyll. Geometry optimization of the $^{D}1$ - ^{2}C adduct for a folded structure is found higher in energy by 0.28 eV. Methanol addition thus causes chlorophyll unfolding because of the suppression of the double bond ^{1}C-^{2}C that was interacting with the magnesium cation in the MeOH-free molecule. Finally, we note that the overall reasoning made for chlorophyll *a* is also qualitatively relevant for pheophytin *a* (Table 3), except that unfolded pheophytin *a* is always found more stable (Table 2). The results in Table 3 illustrate similarities in deprotonation energetics between pheophytin *a* and chlorophyll *a* as both molecules exhibit similar results for each equivalent site. Therefore, methanol addition products should be thermodynamically favored in absence of a barrier. This barrier is likely to be present or higher for pheophytin and could be linked tentatively to the absence of a chain folded form that might enhance the addition through a polarization of the ^{1}C ^{2}C double bond. This is compatible with the calculations on the chain conformation in chlorophyll *a* whose double bond is shown to interact with the charged Mg atom.

Summary

Chlorophyll *a* and pheophytin *a* have been observed by electrospray in the positive (protonated) and negative (deprotonated) modes. While pheophytin *a* is characterized free in the protonated and deprotonated mode, chlorophyll *a* is bound with the solvent in the deprotonated mode. Attention has been focused on the deprotonation sites of both compounds and on the addition of methanol on deprotonated chlorophyll *a*. The localization of the charges has been explored in detail by DFT calculations. In isolated chlorophyll *a* and pheophytin *a*, the acidic deprotonated sites are well identified and separated in energy by E≈0.7eV. One is found on the E cycle at location $C13^{2}$ ($^{D}1$ site) and the other on the propionate chain at $C17^{2}$ (($^{D}2$ site, see figures 1 and 6). On the methanol adduct of chlorophyll, collision experiments have shown that methanol is attached to the phytyl chain. This is confirmed by calculations that yield a 0.6 eV energy for the attachment of $CH_3O^{\cdot}$ to the ^{2}C double bonded carbon of the phytyl chain and H to ^{1}C (see figure 8). It is found that the energetics of pheophytin *a* deprotonation parallels that of chlorophyll *a*, the solvent addition mechanism appears also in calculations similarly.

However experimentally solvent addition is not observed generally for pheophytin *a*. It is inferred that the barrier to solvent addition could be lowered for chlorophyll *a* due to the folding of its phytyl chain and the subsequent interaction with the Mg atom.

The facile deprotonation of pheophytin *a* is linked with its acidic site on the cycle at $C13^2$ whose positive charge in neutral pheophytin would attract electrons. Indeed, through the primary charge separation step in the photoexcited photosystem II of photosynthesis, an electron is transferred from the excited special pair to a pheophytin.

Supplementary Material

The Supplementary material containts the following items :

- Breakdown curves of the fragmentation of deprotonated pheophytin a and b
- The cartesian coordinates of chlorophyll a from MD simulation (Dyn 3 Cluster 4 from table 2)
- The cartesian coordinates of pheophytin a from MD simulation (Dyn 4 Cluster 1 from table 2)
- The cartesian coordinates of the most stable structures of:
  - Deprotonated chlorophyll a,
  - Deprotonated chlorophyll a plus methanol
  - Deprotonated pheophytin a,
  - Deprotonated pheophytin a plus methanol

Acknowledgements

This work was supported by the ANR-21-CE50-0028-01 Electrophylle. We thank GENCI for generous computational resources (project number A0120706913). We thank Dr Michel Broquier (ISMO) for setting up the LCQ mass spectrometer. We thank Dr Manuel Llansola Portoles (I2BC) for constant help and advices on the preparation and purification of Chlorophyll derivatives. We thank Clément Soep (IPCM) for very helpful discussions on collision-induced dissociation in RF traps.

References

1. E. Gruber, C. Kjaer, S. B. Nielsen and L. H. Andersen, Chem.-Eur. J. **25** (39), 9153-9158 (2019).
2. C. Kjær, E. Gruber, S. B. Nielsen and L. H. Andersen, Phys. Chem. Chem. Phys. **22** (36), 20331-20336 (2020).
3. C. Kjær, M. H. Stockett, B. M. Pedersen and S. B. Nielsen, J.Phys.Chem. B **120** (47), 12105-12110 (2016).
4. B. F. Milne, Y. Toker, A. Rubio and S. B. Nielsen, Angew. Chem. Int. Ed. **54** (7), 2170-2173 (2015).
5. B. F. Milne, C. Kjær, J. Houmøller, M. H. Stockett, Y. Toker, A. Rubio and S. B. Nielsen, Angew. Chem. Int. Ed. **55** (21), 6248-6251 (2016).
6. M. H. Stockett, L. Musbat, C. Kjær, J. Houmøller, Y. Toker, A. Rubio, B. F. Milne and S. B. Nielsen, Phys. Chem. Chem. Phys. **17** (39), 25793-25798 (2015).
7. J. B. Zvezdanovic, S. M. Petrovic, D. Z. Markovic, T. D. Andjelkovic and D. H. Andjelkovic, J. Serb. Chem. Soc. **79** (6), 689-706 (2014).
8. J. Hunt, R. Macfarlane, J. Katz and R. C. Dougherty, Proceedings of the National Academy of Sciences **77** (4), 1745-1748 (1980).
9. B. Chait and F. Field, J. Am. Chem. Soc. **106** (7), 1931-1938 (1984).
10. M. Saito, T. Tanabe, K. Noda and M. Lintuluoto, Phys. Rev. A **87** (3), 033403 (2013).
11. S. M. J. Wellman and R. A. Jockusch, Chemistry – A European Journal **23** (32), 7728-7736 (2017).
12. R. Livingston, R. Pariser, L. Thompson and A. Weller, J. Am. Chem. Soc. **75** (12), 3025-3026 (1953).
13. Q. Dumont, M. Bárcenas, H. Dossmann, I. Bailloux, C. Buisson, N. Mechin, A. Molina, F. Lasne, N. S. Rannulu and R. B. Cole, Anal. Chem. **88** (7), 3585-3591 (2016).
14. B. Chiavarino, P. Maitre, S. Fornarini and M. E. Crestoni, J. Am. Soc. Mass. Spectrom. **24** (10), 1603-1607 (2013).
15. T. Müller, A. Badu-Tawiah and R. G. Cooks, Angew. Chem. Int. Ed. **51** (47), 11832-11835 (2012).
16. Y. Hirai, H. Tamiaki, S. Kashimura and Y. Saga, Photoch. Photobio Sci. **8** (12), 1701-1707 (2009).
17. A. Khalyfa, S. Kermasha and I. Alli, J. Agric. Food Chem. **40** (2), 215-220 (1992).

18. P. J. Stephens, F. J. Devlin, C. F. Chabalowski and M. J. Frisch, J. Phys. Chem. **98** (45), 11623-11627 (1994).
19. J. Rezac, J. Fanfrlik, D. Salahub and P. Hobza, J. Chem. Theory Comput. **5** (7), 1749-1760 (2009).
20. M. Korth, M. Pitonak, J. Rezac and P. Hobza, J. Chem. Theory Comput. **6** (1), 344-352 (2010).
21. A. Koster, G. Geudtner, A. Alvarez-Ibarra, P. Calaminici, M. Casida, J. Carmona-Espindola, V. Dominguez, R. Flores-Moreno, G. Gamboa and A. Goursot, in *deMon2k: density of Montreal, version 5.0 the deMon developers, Cinvestav, Mexico City (2018)* (2021).
22. P. Calaminici, A. Alvarez-Ibarra, D. Cruz-Olvera, V. Dominguez-Soria, R. Flores-Moreno, G. Gamboa, G. Geudtner, A. Goursot, D. Mejía-Rodríguez and D. Salahub, Handbook of computational chemistry, 1 (2016).
23. J. Tao, J. P. Perdew, H. Tang and C. Shahi, J. Chem. Phys. **148** (7) (2018).
24. A. D. Becke, J. Chem. Phys. **98** (2), 1372-1377 (1993).
25. P. Calaminici, F. Janetzko, A. M. Köster, R. Mejia-Olvera and B. Zuniga-Gutierrez, J. Chem. Phys. **126** (4) (2007).
26. J. Guan, P. Duffy, J. T. Carter, D. P. Chong, K. C. Casida, M. E. Casida and M. Wrinn, J. Chem. Phys. **98** (6), 4753-4765 (1993).
27. A. M. Köster, J. M. del Campo, F. Janetzko and B. Zuniga-Gutierrez, J. Chem. Phys. **130** (11) (2009).
28. A. M. Köster, R. Flores-Moreno and J. U. Reveles, J. Chem. Phys. **121** (2), 681-690 (2004).
29. R. I. Delgado-Venegas, D. Mejía-Rodríguez, R. Flores-Moreno, P. Calaminici and A. M. Köster, J. Chem. Phys. **145** (22), 224103 (2016).
30. J. Řezáč, J. Comput. Chem. **37** (13), 1230-1237 (2016).
31. MOPAC, (2016).
32. J. Wei, H. Li, M. P. Barrow and P. B. O'Connor, J. Am. Soc. Mass. Spectrom. **24** (5), 753-760 (2013).
33. F. C. Pennington, H. H. Strain, W. A. Svec and J. J. Katz, J. Am. Chem. Soc. **89** (15), 3875-3880 (1967).
34. G. Luis, WMC PhysBio clustering. Available at: https://github.com/luisico/clustering **(Accessed January, 2020)** (2012).
35. W. Humphrey, A. Dalke and K. Schulten, Journal of Molecular Graphics **14** (1), 33-38 (1996).
36. Y. Jiang and R. B. Cole, J. Am. Soc. Mass. Spectrom. **16** (1), 60-70 (2005).